






Research on the IGA Based Multi-hole Wall Plate Structure's Design Technology

Haoyu Wu¹ , Gang Zhao^{1,2}, Xiaoxiao Du³  and Wei Wang^{3,4} 

¹Research Institute of Aero-Engine, Beihang University, Beijing, PR China,
buaawhy@buaa.edu.cn

²Tsinghua University, gangzhao@tsinghua.edu.cn,

³School of Mechanical Engineering and Automation, Beihang University, Beijing, PR China,
duxiaoxiao@buaa.edu.cn

⁴Key Laboratory of Aeronautics Smart Manufacturing, Ministry of Industry and Information Technology, Beijing, PR China, jrrt@buaa.edu.cn

Corresponding author: Wei Wang, jrrt@buaa.edu.cn

Abstract. The isogeometric analysis (IGA) has offered a prospect of integrating CAD and CAE more closely, while the existing CAD models derived from commercial software usually need extra efforts to be made suitable for IGA, which hinders the industry level practice for this budding technology framework. While in certain scenarios, it is highly efficient to generate analysis-suitable models utilizing parametric modeling techniques when the analysis of a series of products with similar geometric features is conducted via IGA. This paper proposes the basic procedures as well as the technology details to realize the IGA based design of multi-hole wall plate structures, which are commonly used in the aerospace industry as external housings and for attaching various components. Traditionally the design procedure was challenging due to the need for repeated modeling and analysis to meet the varied requirements from different sectors. Hence, by using IGA as the analysis tool and combining it with parametric design, the whole process from geometric modeling to performance assessment of multi-hole wall plate structures can be integrated and simplified, enabling the reduction of product development timespan and the improvement of field efficiency.

Keywords: multi-hole wall plates, parametric modeling method, NURBS, iso-geometric analysis, NLIGA

DOI: <https://doi.org/10.14733/cadaps.2024.313-327>

1 INTRODUCTION

For engineers, the traditional product design process involves two critical steps: modeling using Computer-Aided Design (CAD) and performance analysis using the Finite Element Method (FEM). Due to the difference of the geometry representation methods in CAD and FEM, the generation of

analysis model for FEM could be tiresome and time-consuming, especially when the target product is complex and conveys abundant information from different design sectors' requirements, like in the aerospace industry. During the analysis process, if mesh subdivision is necessary, the interaction with the CAD system and mesh re-generation cannot be avoided, accounting for about 80% of overall analysis time [2]. Additionally, for FEM, the mesh is only an approximate representation of the model, resulting in the loss of certain geometric features [3], which also makes the convergence and acquisition of high accuracy results a prolonged process.

To address the issues above, Isogeometric analysis (IGA), proposed by Hughes et al. [9] is a numerical analysis technique that has offered a prospect of integrating CAD and CAE more closely. Same as CAD system, spline technique, such as Non-Uniform Rational B-spline, is employed in IGA for the expression of geometry and field variables, by which the high accuracy and high computational-efficient results can be obtained. Moreover, with the help of IGA, changes to the design can be easily incorporated into the analysis without the frequent need for re-meshing or other modifications, resulting in a more efficient design process. However, a disadvantage of IGA is that it is usually difficult to applied directly to complex models in CAD systems, which are often composed of multiple trimmed and glued surfaces, wherein gaps, overlaps, and non-conforming problems may exist [6]. Modification and generation of models suitable for IGA, consequently, must be implemented, leading to heavy work for geometry fix operation, which hinders the industry level practice for this promising technology.

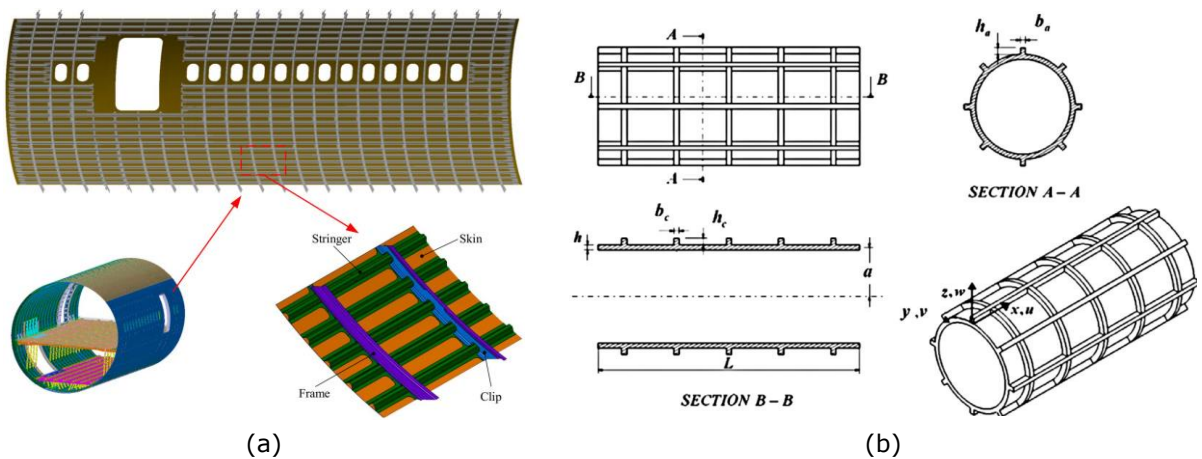


Figure 1: Extensive application of multi-hole wall plate structures: (a) aircraft fuselage [18], (b) stiffened cylindrical shell [7].

Parametric design is a prevailing design approach that is well-suited for designing a sequence of products with similar geometric features. This approach enables users to manipulate one or more parameters, thus facilitating modifications to the geometric model [17]. Notably, in product design, this method shows great capability that various departments can effortlessly implement geometry adjustment without rebuilding the model, significantly reducing the design duration and boosting work efficiency. This method has been widely adopted by engineers in miscellaneous domains owing to its advantages, including architectural design [19], solid rocket engine design [16], and multifunctional cellular material structure design [10].

With the continuous development of CAD and CAE, the IGA-based parametric design platform has received widespread attention and researchers have conducted in-depth research. Hsu et al. [8] proposed an interactive parametric design platform, implemented as Rhino plug-ins, enabling design engineers and analysts to input parameters, generate models, perform analysis, and

visualize results within the same CAD program. In addition, focusing on tunnel design within the Building Information Modeling (BIM) framework, Ninic et al. [14] presented a systematic approach that connects BIM software with IGA for efficient design and analysis. In the similar field, Längst et al. [12] explores the integration of IGA into standard CAD software, providing a unified design toolbox for architectural and engineering projects. Furthermore, Li et al. [13] introduces a user-friendly software platform called HIGA, which integrates geometric modeling, IGA, and post-processing modules for complex hydraulic structures. These studies collectively showcase the benefits of IGA as well as its potential in diverse engineering domains. However, less attention has been paid to the integrated design-analysis approach for models with complex geometric features, such as models with arbitrarily shaped holes.

In the aerospace industry, multi-hole wall plate structures are prevalent due to their frequent use as external housings and their ability to be attached to various components [18, 7], shown in Figure 1. During the general design stage of products such as rocket sections, the main body is typically composed of multi-hole wall plates that serve as the basic structures. However, designing such structures needs to accommodate the different requirements of various sectors, which usually undergo frequent changes, and the resulting modifications must be reflected in the basic structures [4]. The general design sector has to do lot of repeated modeling and analysis work. Even one small change is raised from a certain related sector, the whole process needs to be redone for safety consideration. This situation amplifies the data transferring bottleneck between CAD and FEM, which means the demands for integrated design software is very imperative.

Hence, we have developed a series of methods to implement the IGA-based technique roadmap for designing multi-hole wall plate structures of aerospace products. A parametric modeling interface is utilized to input important design information, and the structure's geometry is segmented into more elementary parts during the modeling process. These segmented elements undergo a special process to make them suitable for IGA. Thus, the IGA-based design process can be performed, aiming at the realization of quick generation and modification of analysis-suitable models and estimation of comprehensive performance, which shortens the product development timespan and improves field efficiency.

This paper is organized as follows. Section 2 begins by introducing the NURBS basic techniques. In Section 3, the parametric modeling method for multi-hole wall plate models that are suitable for IGA is presented. To validate the feasibility of the proposed method, several cases are studied in Section 4. Finally, Section 5 concludes the paper by providing a summary of the research and outlining future research directions.

2 NURBS FUNDAMENTALS

2.1 Trivariate NURBS

The trivariate NURBS is the basis for the elementary geometries' construction. A NURBS volume of degree p in the u direction, degree q in the v direction and degree r in the w direction, respectively, is a trivariate vector-based piecewise rational function of the form

$$\mathbf{S}(u, v, w) = \frac{\sum_{i=0}^n \sum_{j=0}^m \sum_{k=0}^l N_{i,p}(u) N_{j,q}(v) N_{k,r}(w) \omega_{i,j,k} \mathbf{P}_{i,j,k}}{\sum_{i=0}^n \sum_{j=0}^m \sum_{k=0}^l N_{i,p}(u) N_{j,q}(v) N_{k,r}(w) \omega_{i,j,k}} \quad (2.1)$$

The $\mathbf{P}_{i,j,k}$ form a tridirectional control net, the $\omega_{i,j,k}$ are the weights, and the $N_{i,p}(u)$, $N_{j,q}(v)$ and $N_{k,r}(w)$ are the nonrational B-spline basis functions defined on the knot vectors

$$\begin{aligned}
 U &= \left\{ \underbrace{0, \dots, 0}_{p+1}, u_{p+1}, \dots, u_{\alpha-p-1}, \underbrace{1, \dots, 1}_{p+1} \right\} \\
 V &= \left\{ \underbrace{0, \dots, 0}_{q+1}, v_{q+1}, \dots, v_{\beta-q-1}, \underbrace{1, \dots, 1}_{q+1} \right\} \\
 W &= \left\{ \underbrace{0, \dots, 0}_{r+1}, w_{r+1}, \dots, w_{\gamma-r-1}, \underbrace{1, \dots, 1}_{r+1} \right\}
 \end{aligned} \tag{2.2}$$

where $\alpha = n + p + 1$, $\beta = m + q + 1$ and $\gamma = l + r + 1$.

2.2 Cylindrical Intersecting Curve Fitting

In the process of parametric modeling for multi-hole wall plates, it is essential to partition the wall plate with holes into several basic elements of hexahedral topology to generate a model suitable for isogeometric analysis [1]. The partition-fitting-modeling process, taking a wall plate with a circular hole as an example, is described briefly in this section and the following one.

The first task of the segmentation process is to split the contour curve of the hole, whose mathematical nature is an intersecting curve composed of two mutually perpendicular cylinders with intersecting axes. For such cylindrical intersecting curves, the parametric equation is

$$\begin{cases} x = x(\varphi) = R_2 \cos(\varphi) \\ y = y(\varphi) = \pm \sqrt{R_1^2 - R_2^2 \cos^2(\varphi)} & \varphi \in [0, 2\pi] \\ z = z(\varphi) = R_2 \sin(\varphi) \end{cases} \tag{2.3}$$

where R_1 , R_2 are the radii of the two cylinders respectively.

In this paper, we divide the intersecting curve into four parts, which means that segmentation is implemented at the points where $\varphi = 45^\circ, 135^\circ, 225^\circ, 315^\circ$ according to Equation (2.3), also shown as point A, B, C and D in Figure 2(a). Each part is fitted with a cubic NURBS curve, using the global curve interpolation method with specified end derivatives, as described in [15]. Every derivative whereby gives rise to one additional knot and control point, and hence to one additional linear equation. Data points $Q_k, k = 0, \dots, n$ are uniformly sampled on the parameter curve, with D_0 and D_n representing the end derivatives. To simplify the implementation and at the same time guarantee the needed precision, we set $n = 4$ and assign all control point weights a value of 1.

Using chord length method, let d be the total chord length

$$d = \sum_{k=1}^n |Q_k - Q_{k-1}| \tag{2.4}$$

Then

$$\bar{u}_0 = 0, \bar{u}_n = 1, \quad \bar{u}_k = \bar{u}_{k-1} + \frac{|Q_k - Q_{k-1}|}{d}, \quad k = 1, \dots, n-1 \tag{2.5}$$

The knots are

$$\begin{aligned}
 u_0 = \dots = u_3 = 0, \quad u_{n+3} = \dots = u_{n+6} = 1 \\
 u_{j+3} = \bar{u}_j, \quad j = 1, 2, \dots, n-1
 \end{aligned} \tag{2.6}$$

Based on the data points given before, $n + 1$ equations can be obtained

$$\mathbf{Q}_k = \mathbf{C}(\bar{u}_k) = \sum_{i=0}^{n+2} N_{i,3}(\bar{u}_k) \mathbf{P}_i \quad (2.7)$$

Two additional equations are given below according to the expressions of end derivatives

$$-\mathbf{P}_0 + \mathbf{P}_1 = \frac{u_1}{3} \mathbf{D}_0 \quad (2.8)$$

$$-\mathbf{P}_{n+1} + \mathbf{P}_{n+2} = \frac{1 - u_{n+2}}{3} \mathbf{D}_n \quad (2.9)$$

Inserting Equation (2.8) and (2.9) into Equation (2.7) as the second and next to last equations, respectively, yields the fitting result, shown in Figure 3(a), where we assume that $R_1 = 100 \text{ mm}$,

$R_2 = 80 \text{ mm}$ and the hole is located at the center of the wall plate.

2.3 Surface Fitting

After successfully fitting the intersecting curve, the trimmed outer surface of the cylinder, taking the surface 1 as an example, needs to be fitted, as shown in Figure 2(a).

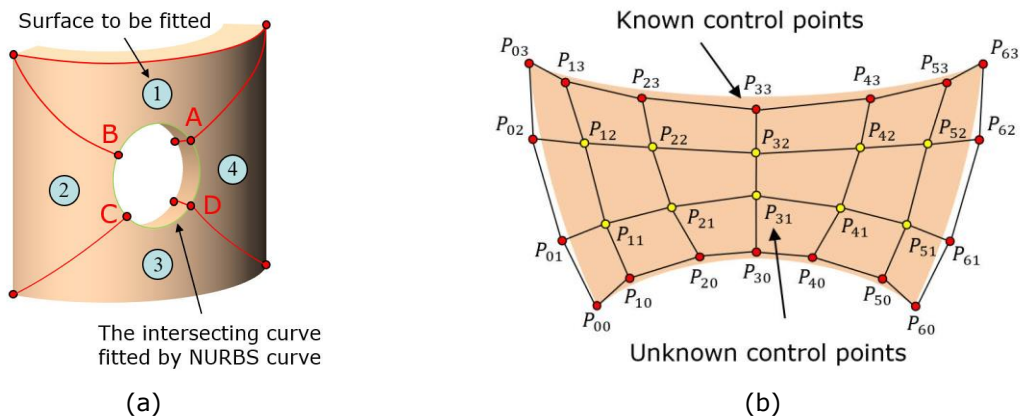


Figure 2: Wall plate with a round hole: (a) curves and surfaces to be fitted, (b) schematic diagram of surface fitting, with red dots representing known control points and yellow ones are unknown.

Surface fitting is implemented by global surface interpolation method, using NURBS bicubic surface. Data points $Q_{k,l}$, $k = 0, \dots, n$, $l = 0, \dots, m$ are sampled uniformly on the cylindrical sidewall surface. In order to inherit the fitting result described in Section 2.2, here $n = 6$ according to Equation (2.7); on the other hand, the segmentation curves are all cylindrical helices, which can be approximated by a cubic rational Bézier curve, so $m = 3$. Again, the first order of business is to obtain reasonable values for the \bar{u}_k, \bar{v}_l and the knot vectors U and V . Parameters $\bar{u}_0^l, \dots, \bar{u}_n^l$ for each l are computed using the chord length method, and then each \bar{u}_k is acquired by averaging across all \bar{u}_k^l , $l = 0, \dots, m$, as shown in Equation (2.10); the \bar{v}_l are analogous.

$$\bar{u}_k = \frac{1}{m+1} \sum_{l=0}^m \bar{u}_k^l \quad k = 0, \dots, n \tag{2.10}$$

Knot vectors U and V are inherited directly from the ones of the contour curves located on the surface boundary, of which the NURBS geometric representation is already processed, i.e., an arc, two cylindrical helices [11], and the result of curve fitting.

Equations for surface interpolation, subsequently, are given below.

$$\mathbf{Q}_{k,l} = \frac{\sum_{i=0}^n \sum_{j=0}^m N_{i,p} \bar{u}_k N_{j,q} \bar{v}_l w_{i,j} \mathbf{P}_{i,j}}{\sum_{i=0}^n \sum_{j=0}^m N_{i,p} \bar{u}_k N_{j,q} \bar{v}_l w_{i,j}} \tag{2.11}$$

Let

$$\mathbf{R}_{k,l}^w = \sum_{i=0}^n \sum_{j=0}^m N_{i,p} \bar{u}_k N_{j,q} \bar{v}_l w_{i,j} \mathbf{Q}_{k,l} \tag{2.12}$$

and

$$\mathbf{P}_{i,j}^w = w_{i,j} \mathbf{P}_{i,j} \tag{2.13}$$

Therefore, Equation (2.10) can be written as

$$\mathbf{R}_{k,l}^w = \sum_{i=0}^n N_{i,p} \bar{u}_k \left(\sum_{j=0}^m N_{j,q} \bar{v}_l \mathbf{P}_{i,j}^w \right) \tag{2.14}$$

The essence of solving Equation (2.14) is to perform two successive curve interpolation operations in four-dimensional space. Fitting result is presented in Figure 3(b).

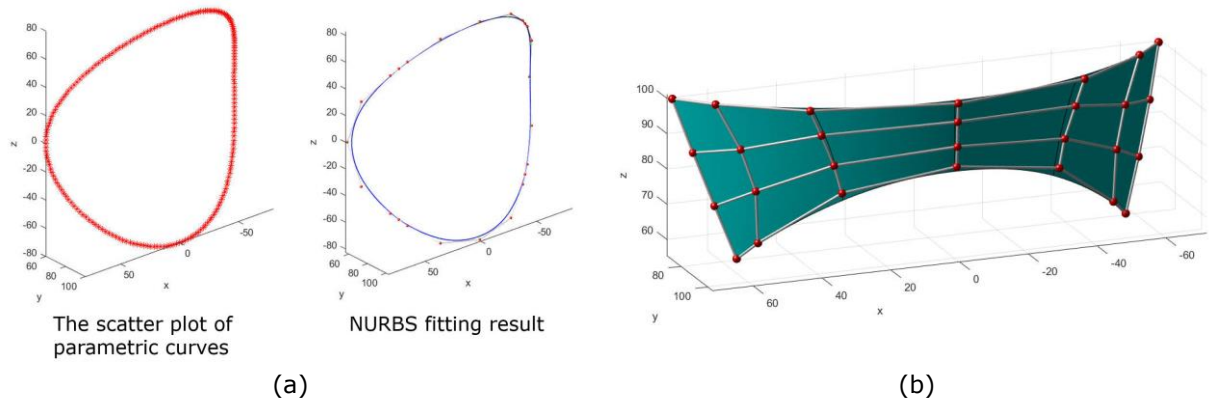


Figure 3: Fitting results: (a) cylindrical intersecting curve, (b) surface 1 in Figure 2(a).

3 PARAMETRIC MODELING METHOD

Multi-hole wall plates are generally regularly wrapped around the outer surface of the aerospace product to help the product withstand external loads, such as bending or torsion. In addition,

conforming elements, shown in Figure 4, are often used in the meshing process of IGA, facilitating the stiffness matrix assembly of computation. Since the arrangement pattern of the wall plates is in accordance with the characteristics of the conforming elements, it is reasonable and effective to conduct parametric design and mechanical analysis based on the conforming elements.

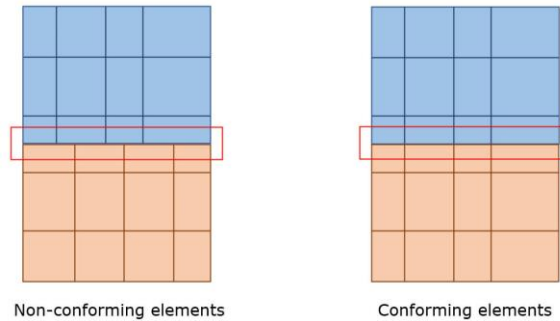


Figure 4: Non-conforming elements and conforming elements

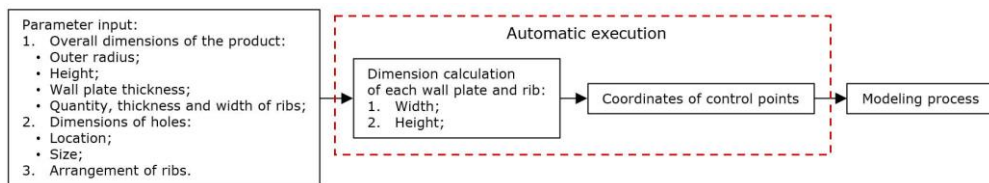


Figure 5: The illustration of automatic parameter processing during the modeling procedure of cylindrical wall plate structure.

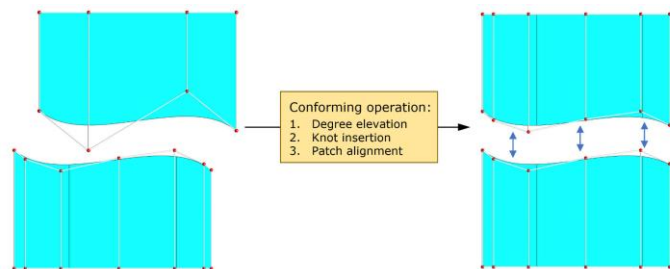


Figure 6: Conforming operation: degree elevation, knot insertion and patch alignment.

The parametric modeling process of multi-hole wall plates is briefly described below, which is clearly shown in Figure 7.

1. Parameter input: users input overall dimensions of the product, and the location as well as size of the holes, respectively, according to the design requirements.
2. NURBS volume modeling: the parametric modeling program is similar to a "black box", which will automatically calculate the position and size of each basic elements according to the design requirements. The key information, such as control point coordinates, is derived during the modeling process, which is illustrated in Figure 5, taking the cylindrical wall plate structure for instance. Firstly, the wall plates without holes and the ribs, same as the NURBS volume, which is hexahedral in topology, can be modeled directly. Secondly, for the ones with holes, the program will automatically figure out which wall plate the hole is located on and segment it into several basic hexahedral elements, then the fitting

operation is whereby performed. Finally, NURBS volume models for analysis are obtained based on the open-source framework NLIGA [5].

3. Assembly: the NURBS volume models need to be assembled according to the dimensional parameters and design requirements after modeling process. The assembly procedure can be regarded as conforming operation, which is automatically implemented according to the dimensional parameters and design requirements after modeling process, including:
 - (1) Degree elevation: traverse each wall plate model to find the model with highest degree in direction u , v and w , and perform degree elevation on the other models to make sure that all models have the same degree.
 - (2) Knot insertion: during the traversal, the merge set is taken for all knot vectors. Perform knot insertion operations to keep the knot vectors consistent for all models.
 - (3) Patch alignment: set the coordinates for all wall plate models, which means that each wall plate model is automatically moved to the specified position in order to achieve patch alignment.
4. Analysis: material properties and mechanical boundary conditions are set for the mechanical analysis of the model, providing guidance for the adjustment of design parameters and performance optimization of the wall plate structure.

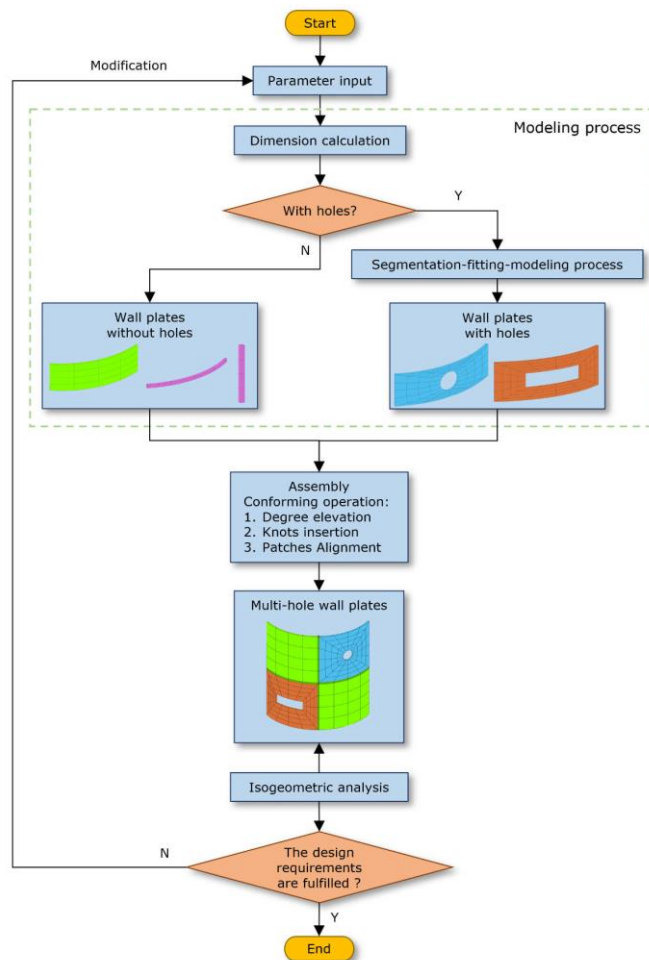


Figure 7: Flowchart of the IGA based parametric design program.

All models are stored into a one-dimensional array, which facilitates the temporary addition or removal of holes and quick modeling. A wall plate model without holes is stored first, and if a certain wall plate needs to be perforated, it will be replaced by one with square or round holes, enabling quick modification and re-modeling, as shown in Figure 8.

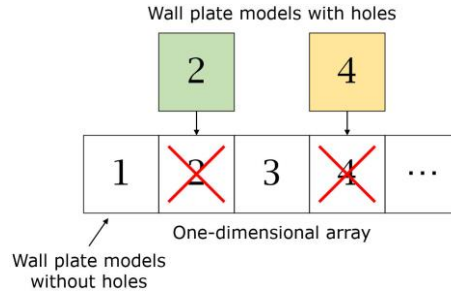


Figure 8: The method for model information storage, where the green square represents the wall plate with square holes, and the yellow one represents the wall plate with round holes.

4 CASE STUDY

4.1 Linear Elasticity Problem Based on IGA

Formulations for 3D linear elasticity problems based on isogeometric analysis method are briefly discussed in this section, which serve as the theoretical basis for the following section. Given a physical domain $\Omega \rightarrow \mathbb{R}^3$ with boundary $\Gamma = \partial\Omega$, establish the strong form of governing equations as

$$\nabla \sigma + \mathbf{b} = \mathbf{0}$$

$$\epsilon = \frac{1}{2} \nabla \mathbf{u} + \nabla^T \mathbf{u} \quad (4.1)$$

$$\sigma = \mathbf{D} : \epsilon$$

The Dirichlet boundary conditions and Neumann boundary conditions are introduced below

$$\begin{aligned} \mathbf{u} &= \bar{\mathbf{u}} \quad \text{on } \Gamma_D \\ \sigma \cdot \mathbf{n} &= \bar{\mathbf{p}} \quad \text{on } \Gamma_N \end{aligned} \quad (4.2)$$

where $\bar{\mathbf{u}}$ refer to prescribed boundary displacements and $\bar{\mathbf{p}}$ refer to the tractions, respectively.

According to the principle of virtual work, Equation (4.1) can be written as

$$\int_{\Omega} \sigma : \delta \epsilon \, d\Omega - \left(\int_{\Omega} \bar{\mathbf{b}} \cdot \delta \mathbf{u} \, d\Omega + \int_{\Gamma_N} \bar{\mathbf{p}} \cdot \delta \mathbf{u} \, d\Gamma \right) = 0 \quad (4.3)$$

Moreover, discretization of the whole model is implemented for calculation, such that the geometry \mathbf{x} on a certain element is described as

$$\mathbf{x} = \sum_{i=1}^{ncp} R_i \mathbf{P}_i \quad (4.4)$$

where R_i means NURBS basis function, \mathbf{P}_i means control points and ncp means the number of control points, respectively. The displacement \mathbf{u} and its variation $\delta \mathbf{u}$, following the isogeometric concept, are expressed as

$$\mathbf{u} = \sum_{i=1}^{ncp} R_i \mathbf{d}_i$$

$$\delta \mathbf{u} = \sum_{i=1}^{ncp} R_i \delta \mathbf{d}_i$$
(4.5)

Global stiffness equation is acquired by substituting Equation (4.5) into Equation (4.3)

$$\mathbf{Kd} = \mathbf{p}$$
(4.6)

in which \mathbf{K} stands for stiffness matrix, \mathbf{d} stands for displacement vector to be calculated and \mathbf{p} stands for load vector. Consequently, the performance of the product can be substantiated via the estimation of the solving result.

4.2 Case 1: Cylindrical Multi-hole Wall Plate Structure

According to the parametric modeling method in Section 3, a cylindrical wall plate model is built, which is widely used around the outer surface of the rocket. Important design parameters are listed in Table 1 below.

Parameters	Symbols	Values
Outer radius of the structure	R	600 (mm)
Height	H	780 (mm)
Wall plate thickness	t	30 (mm)
Number of axial ribs	n_a	6
Number of circumferential ribs	n_c	2
Width of axial ribs	w_a	4 (°)
Width of circumferential ribs	w_c	30 (mm)
Thickness of all ribs	t_r	25 (mm)

Table 1: Overall dimensions of the cylindrical wall plate structure.

Assuming a uniform arrangement of ribs, input the above parameters into the program to obtain a model without holes, as shown in Figure 9(a). A detailed illustration of dimension calculation for a certain wall plate is presented. For the wall plate located in row i and column j , as shown in Figure 5, the dimensions to be calculated include its height h , width w , and position h_1 , h_2 , w_1 , w_2 .

Here, assuming a uniform distribution of the ribs, the height h is calculated as

$$h = \frac{H - n_c \cdot w_c}{n_c + 1}$$
(4.7)

At the same time, the width w is calculated as

$$w = \frac{2\pi}{n_a} - w_a$$
(4.8)

Therefore, height of bottom and top of wall plate is acquired

$$h_1 = i \cdot h + w_c$$
(4.9)

$$h_2 = h_1 + h$$
(4.10)

Similarly, angular coordinates of the wall plate can be expressed as

$$w_1 = j \cdot \frac{2\pi}{n_a}$$
(4.11)

$$w_2 = w_1 + w \quad (4.12)$$

Combining the above dimensioning process with the key dimensions in Table 1, the control point coordinates of the model can be obtained.

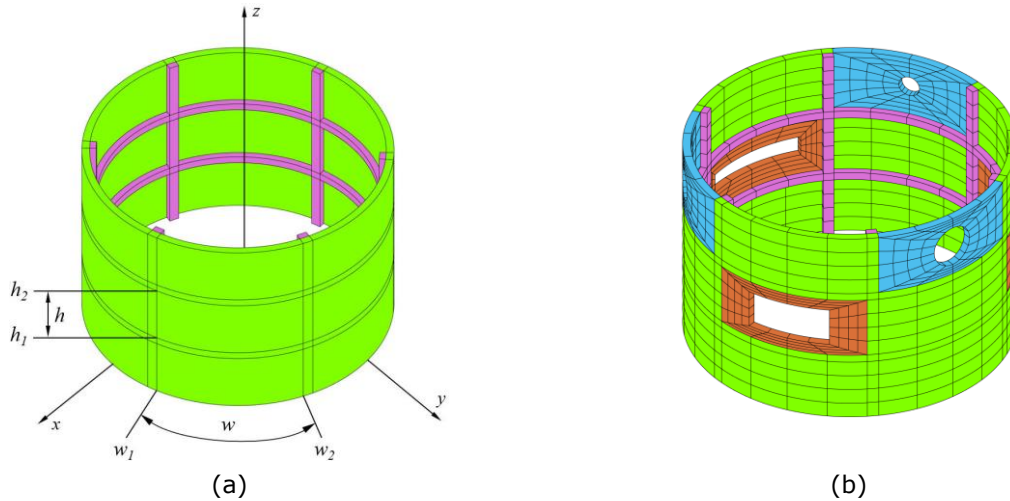


Figure 9: The cylindrical wall plate structure: (a) with no holes, (b) with square and round holes.

The following parameters can be input if square holes and round holes are desired (supposing that the holes are centered in the wall plates). A new model is obtained after re-modeling process, shown in Figure 9(b).

Parameters	Symbols	Values
Circumferential and Z-axis coordinates of square holes	θ_{sqr}, z_{sqr}	28 ($^{\circ}$), 390 (mm); 148 ($^{\circ}$), 390 (mm); 268 ($^{\circ}$), 390 (mm);
Width of square holes	w_{sqr}	30; 20; 40 ($^{\circ}$)
Height of square holes	h_{sqr}	150; 100; 80 (mm)
Circumferential and Z-axis coordinates of round holes	θ_{rnd}, z_{rnd}	88 ($^{\circ}$), 660 (mm); 208 ($^{\circ}$), 660 (mm); 328 ($^{\circ}$), 660 (mm);
Radii of round holes	r_{rnd}	80; 40; 60 (mm)

Table 2: Dimensions of the hole features.

In order to analyze the axial load carrying capacity of the structure, we fixed the bottom of the model and applied 100 MPa pressure on the top, based on the assumption of elastic material. Figure 10(a) shows the results of the isogeometric analysis, while Figure 10(b) shows the results from ABAQUS.

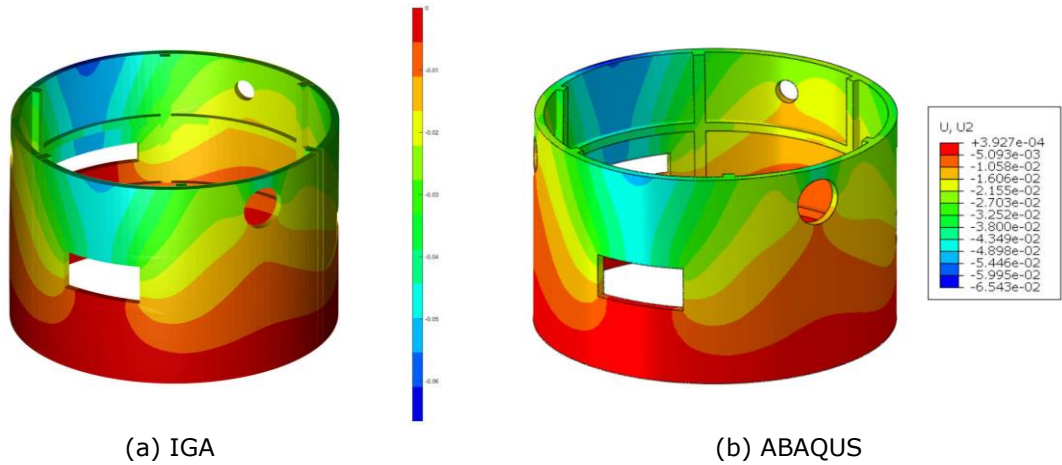


Figure 10: Analysis result of cylindrical wall plate structure using different method.

4.3 Case 2: Fuselage with Round Holes

To illustrate the repeatability of the method, we also applied it to the modeling construction of an aircraft fuselage, as shown in Figure 11. The key dimensions to be entered are the fuselage length, the outer radius of the circular plate, the height of the flat plate, the hole size (located in the center of the wall plates), and the width of ribs (uniformly distributed), illustrated in Table 3.

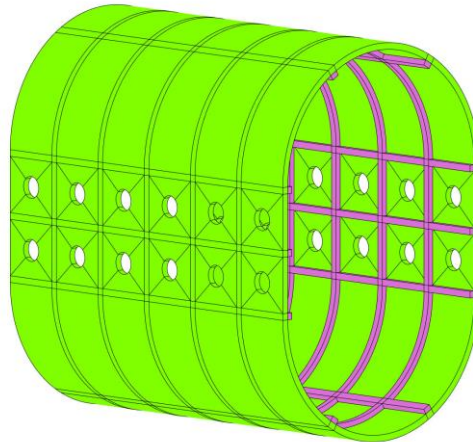


Figure 11: Fuselage with round holes.

Performance analysis is then conducted. Here we fixed the left end of the model and applied a 200MPa surface traction along Z axis on the right end, based on the assumption of elastic material. Figure 12(a) shows the results of the isogeometric analysis, while Figure 12(b) shows the results from ABAQUS.

<i>Parameters</i>	<i>Symbols</i>	<i>Values</i>
Length	<i>L</i>	1800 (mm)
Outer radius of the circular plate	<i>R</i>	600 (mm)

Height of the flat plate	H	600 (mm)
Wall plate thickness	t	30 (mm)
Number of circular axial ribs	n_{ca}	4
Number of circular circumferential ribs	n_{cc}	5
Width of circular axial ribs	w_{ca}	4 ($^{\circ}$)
Width of circular circumferential ribs	w_{cc}	30 (mm)
Number of flat axial ribs	n_{fa}	3
Number of flat circumferential ribs	n_{fc}	5
Width of flat axial ribs	w_{fa}	30 (mm)
Width of flat circumferential ribs	w_{fc}	30 (mm)
Thickness of all ribs	t_r	25 (mm)
Radius of round holes	r_{rnd}	50 (mm)

Table 3: Overall dimensions of the fuselage.

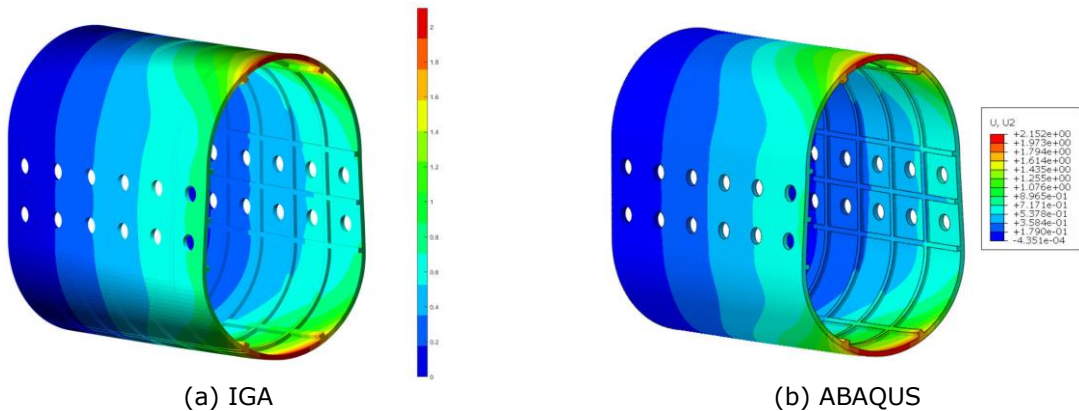


Figure 12: Analysis result of fuselage using different method.

<i>Youngs modulus</i> 3×10^6	<i>Scales</i>	<i>Case</i>	<i>Load (MPa)</i>	<i>Methods</i>	<i>Number of meshes</i>	<i>Maximum vertical displacement magnitude (mm)</i>
<i>Poisson ratio</i> 0.6	1 : 1	1	100	IGA	120	6.747×10^{-2}
				FEA	84270	6.543×10^{-2}
		2	200	IGA	452	2.249
				FEA	301812	2.152

Table 4: Experiment parameters and the result comparison between IGA and FEA.

Referring to Table 4, the results of IGA are found in good coincidence with those of ABAQUS. However, the number of meshes used in IGA is far less than the one in FEA, highlighting the high efficiency and better convergence behavior of IGA.

5 CONCLUSION

This paper put forwards an IGA-based design approach for multi-hole wall plate structures, which presents the conception of integrating modeling & analysis in one single software environment, enabling engineers to rapidly and effectively make preliminary assessments of product performance and expeditiously re-model it in accordance with design specifications. The case studies prove the effectiveness and practicality of the method. Moreover, the paper shows that although using IGA as a basic pattern for product design still needs more efforts even breakthroughs in geometry modeling theory, it can exert prowess in circumstances where the product's shape features are comparatively stable and regular, which will provide practical experiences for the implementation of CAD/CAE integrating software. Note that in the methods provided in this paper, the fitting accuracy may not reach the expected requirements using interpolation if holes and surfaces have more complex geometric features. Future work, therefore, will focus on improving the fitting accuracy and preserving as many local details as possible.

Haoyu Wu, <https://orcid.org/0009-0009-3539-009X>

Xiaoxiao Du, <https://orcid.org/0000-0002-2324-1005>

Wei Wang, <https://orcid.org/0000-0002-5089-0000>

6 ACKNOWLEDGEMENT

This research is supported by National Science Foundation of China (Project Nos. 52175213, 61972011, 62102012) and China Postdoctoral Foundation (Project No. 2021M690294).

REFERENCES

- [1] Chen, L.; Bu, N.; Jin, Y.; Xu, G.; Li, B.: Construction of IGA-suitable Volume Parametric Models by the Segmentation–Mapping–Merging Mechanism of Design Features, *Computer Aided Design*, 146, 2022, 103228. <https://doi.org/10.1016/j.cad.2022.103228>
- [2] Cottrell, J. A.; Hughes, T. J. R.; Bazilevs, Y.: *Isogeometric Analysis: Toward Integration of CAD and FEA*, John Wiley & Sons, 2009. <https://doi.org/10.1002/9780470749081>
- [3] Cottrell, J. A.; Reali, A.; Bazilevs, Y.; Hughes, T. J. R.: Isogeometric analysis of structural vibrations, *Computer methods in applied mechanics and engineering*, 195(41-43), 2006, 5257-5296. <https://doi.org/10.1016/j.cma.2005.09.027>
- [4] Dostaler, I.: Avoiding rework in product design: evidence from the aerospace industry, *International Journal of Quality & Reliability Management*, 27(1), 2010, 5-26. <https://doi.org/10.1108/02656711011009281>
- [5] Du, X.; Zhao, G.; Wang, W.; Guo, M.; Zhang, R.; Yang, J.: NLIGA: A MATLAB framework for nonlinear isogeometric analysis, *Computer Aided Geometric Design*, 80, 2020, 101869. <https://doi.org/10.1016/j.cagd.2020.101869>
- [6] Du, X.; Zhao, G.; Wang, W.; Guo, M.; Zhang, R.; Yang, J.: Triangular and Quadrilateral Bézier Discretizations of Trimmed CAD Surfaces and its Application to the Isogeometric Analysis, *Computer-Aided Design & Applications*, 18(4), 2021, 738-759. <https://doi.org/10.14733/cadaps.2021.738-759>
- [7] Farahani, H.; Azarafza, R.; Barati, F.: Mechanical buckling of a functionally graded cylindrical shell with axial and circumferential stiffeners using the third-order shear deformation theory, *Comptes Rendus Mécanique*, 342(9), 2014, 501-512. <https://doi.org/10.1016/j.crme.2014.04.001>
- [8] Hsu, M.-C.; Wang, C.; Herrema, A. J.; Schillinger, D.; Ghoshal, A.; Bazilevs, Y.: An interactive geometry modeling and parametric design platform for isogeometric analysis, *Computers & Mathematics with Applications*, 70(7), 2015, 1481-1500. <https://doi.org/10.1016/j.camwa.2015.04.002>

- [9] Hughes, T. J. R.; Cottrell, J. A.; Bazilevs, Y.: Isogeometric analysis: CAD, finite elements, NURBS, exact geometry and mesh refinement, *Computer Methods in Applied Mechanics and Engineering*, 194(39), 2005, 4135-4195. <https://doi.org/10.1016/j.cma.2004.10.008>
- [10] Jones, A.; Leary, M.; Bateman, S.; Easton, M.: Parametric design and evaluation of TPMS-like cellular solids, *Materials & Design*, 221, 2022, 110908. <https://doi.org/10.1016/j.matdes.2022.110908>
- [11] Juhász, I.: Approximating the helix with rational cubic Bézier curves, *Computer-Aided Design*, 27(8), 1995, 587-593. [https://doi.org/10.1016/0010-4485\(95\)99795-A](https://doi.org/10.1016/0010-4485(95)99795-A)
- [12] Längst, P.; Bauer, A. M.; Michalski, A.; Lienhard, J.: The Potentials of Isogeometric Analysis Methods in Integrated Design Processes, *Proceedings of IASS Annual Symposia*, 2017(8), 2017, 1-10. <https://www.ingentaconnect.com/content/iass/piass/2017/00002017/00000008/art00015>
- [13] Li, M.; Chen, Y.; Zhang, M.; Yang, L.; Lian, H.; Bordas, S. P. A.; Kong, R.: Platform for isogeometric analysis of complex hydraulic structures, *Automation in Construction*, 152, 2023, 1048-82. <https://doi.org/10.1016/j.autcon.2023.104882>
- [14] Ninic, J.; Giang Bui, H.; Meschke, G.: Parametric Design and Isogeometric Analysis of Tunnel Linings within the Building Information Modelling Framework, *CEUR Workshop Proceedings*, 2394, 2019. <https://nottingham-repository.worktribe.com/output/2294653>
- [15] Piegl, L.; Tiller, W.: *The NURBS book*, Springer Berlin, Heidelberg, 1997.
- [16] Ren, J.; Bao, F.-T.; Wei, R.; Dai, L.; Zhang, J.: Research on The Parametric Solid Modeling Method of Solid Rocket Motor for Multiphysics Simulation. 2022 13th International Conference on Mechanical and Aerospace Engineering (ICMAE), IEEE, 2022, 264-269. <https://doi.org/10.1109/ICMAE56000.2022.9852841>
- [17] Roller, D.: An approach to computer-aided parametric design, *Computer-Aided Design*, 23(5), 1991, 385-391. [https://doi.org/10.1016/0010-4485\(91\)90033-S](https://doi.org/10.1016/0010-4485(91)90033-S)
- [18] Wang, Z.; Li, D.; Shen, L.; Dong, X.; Zhai, Y.: Multi-objective optimisation of assembly fixturing layout for large composite fuselage panel reinforced by frames and stringers, *The International Journal of Advanced Manufacturing Technology*, 2023, 1-16. <https://doi.org/10.1007/s00170-022-10776-1>
- [19] Yuan, Z.; Sun, C.; Wang, Y.: Design for Manufacture and Assembly-oriented parametric design of prefabricated buildings, *Automation in Construction*, 88, 2018, 13-22. <https://doi.org/10.1016/j.autcon.2017.12.021>